Development of Solar Spectroradiometer for Meteorological Observation

LIU Liying[1], ZHENG Feng[2,*], ZHANG Guoyu[1], XU Yigang[2], Yang Liyan[2], LV Wenhua[3], BIAN Zeqiang[3], CHONG Wei[3], LI Ye[1]

1. Changchun University of Science and Technoloy, Changchun, 130000, China;

2. Jiangsu Radio Scientific institute Co., LTD, Wuxi, 214127, China;

3. CMA MeteorologicalObservation Centre, Beijing, 100081, China

Abstract: A new generation of solar spectroradiometerhas been developed by CUST/JRSI to improve solarirradiance observation data underhyperspectral resolution. It is based on the grating spectroradiometer with a back-thinned CCD linear image sensor and is operated in a hermetically sealed enclosure. The solar spectroradiometer is designed to measure the solar spectral irradiance from 300nm to 1100nm wavelength range with the spectral resolution of 2nm (the full width at half maximum). The optical bench is optimized to minimize stray light. The Peltier device is used to stabilize the temperature of CCD sensor to 25℃, while the change of temperature of CCD sensor is controlled to ±1℃ by the dedicated Peltierdriver and control circuit.

Key words: Solar Irradiance Observation, Spectroradiometer, Hyperspectral Resolution

1 Introduction

In the past, meteorological solar irradiance observation was typically required for several widely spaced broad spectral channels by optical band pass filter. In 2003, NASA has achieved the SORCE (Solar Radiation and Climate Experiment) project mission successfully, which has included the SIM (Spectral Irradiance Monitor) system. The SIM observations are improving the understanding of solar activity and generating new inquiry regarding how and why variability occurs and how it affects atmosphere and climate. In NASA's technical report, in order to achieve a comprehensive understanding of the sun's influence on the atmosphere, it is crucial that the datasets of solar irradiance include detailed and specific wavelength information[1,2]. In Japan, EKO Instruments Ltd. has launched a series of rugged spectroradiometer products (MS7XX series) for meteorological solar irradiance observation outdoors in recent ten years[3,4]. In 2013, PMOD/WRC has finished a PSR (Precision Solar Spectroradiometer) project. Subsequently, a small series of PSR has been manufactured for solar spectral irradiance observation[5,6]. In 2014, the JRSI (Jiangsu Radio Scientific Institute Co., Ltd) cooperated with CUST (Changchun University of Science and Technology) and CMA (Meteorological Observation Centre) to start up the solar spectroradiometer project supported by Meteorology Industry Research Special Funds for Public Welfare Projects in China[7]. In this paper, the results and key features of solar spectroradiometer are expounded and discussed.

2 Schematic of Optical Bench

Theoptical bench of spectroradiometer can be regarded as the engine in the instrument system. Each component and matching between components will have influence on the performance[8,9,10]. There are many different commercial spectrograph manufacturers on the international market, such as Avantes, B&W Tek, BaySpec, Hamamatsu, Horiba JobinYvon, Labsphere, JETI, Ocean Optics, Shimadzu, StellarNet, Zeiss/Tec5 and so on. There are also some commercial spectrograph products in domestic market, but the state of the art in domestic is comparatively lower than the one of abroad manufactures. Some commercial spectrograph manufacturers can provide spectrograph OEM module, but it is very difficult to customize characteristic deeply. Thus, the optical bench of spectroradiometer has been designed and optimized all by ourselves.

Thereare three basic topological forms of optical bench for the grating spectrograph, which are illustrated in figure1-a), 1-b) and 1-c) respectively. The CHG form has been selected for two reasons. One is that there are less optical components than the other two forms. Less optical surfaces could reduce the stray light (the stray light is formed by reflection between optical surfaces). It is helpful to improve the signal-to-noise ratio of the system. The other is that less optical components make this optical bench have less geometric parameters for alignment.

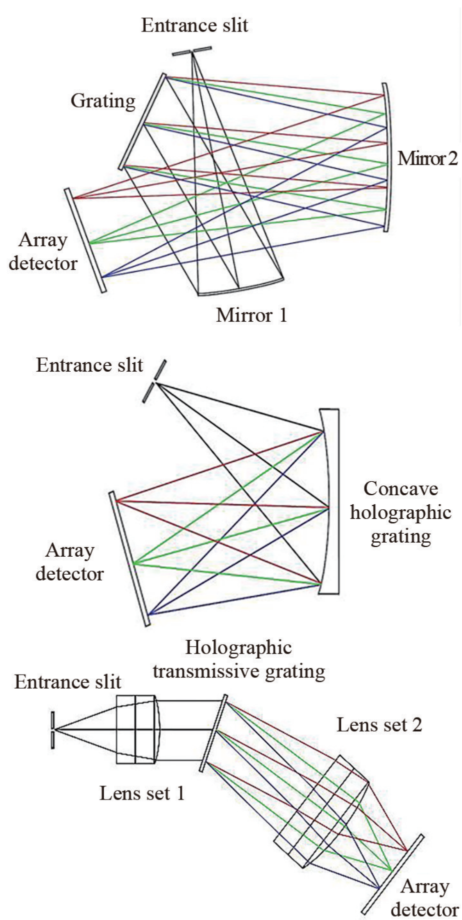

Fig. 1 a) PRG (Plane Reflective Grating). b) CHG (Concave Holographic Grating). c) PTG (Plane Transmissive Grating).

The schematic diagram of spectrograph based on concave grating is shown in Figure 2. There are only 4 key elements in the optical system: the first one is the concave grating, the second one is the CCD linear image sensor, the third one is the order sorting filter and the last one is the mechanical slit connected to the end of optical fiber.

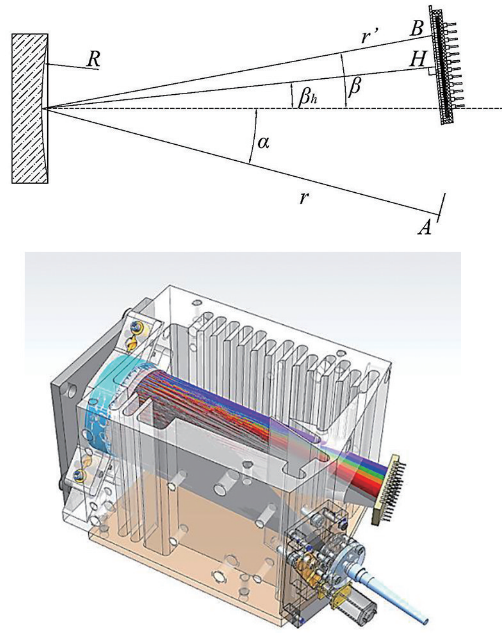

Fig. 2 Schematic diagram of optical bench. b) Designed 3D model of optical bench.

3 Key Features of Optical Bench

The keyfeatures of spectrograph and features of key components are shown in detail as follows.

The first key feature is imaging characteristic of optical bench. The optical bench is an imaging system which maps a plurality of monochromatic images of the incident slit onto the plane of detector. Thus the width of incident slit sets an ultimate limit on the resolution of the spectrograph. So the image aberrations of the optical bench impose an important limit on the spectral resolution of spectrograph. After investigation, the HORIBA's Type IV aberration corrected flat field & imaging gratings has been selected. This grating is designed to focus a spectrum onto a plane surface making it ideal for use with linear array detector. These gratings are produced with grooves that are neither equispaced nor parallel, and are computer optimized to form near-perfect image of the incident slit on the detector plane. Figure3 shows the spectral slit images on the area of image sensor plane using the mercury- argon lamp source. The slit images in center are near-perfect with the height of 1000um. The slit images still have some astigmatism and coma on both sides, which make the shape of silt images have a small geometric distortion.

Fig. 3 Spectral slit images on the area of image sensor plane

The second key feature is the detector performance and the matching degree between image and detector. The size of incident slit determines the total optical flux entering into the optical bench, which in turn sets a limit on the sensitivity of the spectrograph. The width of the slit is determined by spectral resolution requirement and the height of the slit is confirmed by the height of pixel of array detector. The Hamamtsu back-thinned CCD linear image sensor has been selected and its pixel size is 14um×1000um. For this CCD sensor, a resistive gate structure is used in the photosensitive area. The back of the resistive gate is thinned, which enables the CCD to achieve high quantum efficiency over a wide spectral range in the same manner as ordinary back-thinned CCDs. Furthermore, the photosensitive area has a structure that suppresses the etaloning (an interference phenomenon that is characteristic of back-thinned CCDs) that occurs in near infrared wavelengths. These image sensors use a resistive gate structure that allows a high-speed transfer. Each pixel has a lengthwise size needed by spectrograph. There are two typical sources of NL (Non-Linearity) from CCD's characteristics. One NL source is the temperature dependence. The Peltier device is used to stabilize the temperature of CCD sensor to 25℃, while the change of temperature of CCD sensor is controlled to ±1℃ by the dedicated Peltier driver and control circuit. So the issue of temperature dependence can be controlled well. Another NL source is the integration time dependence. This issue will be corrected by gray level measurement.

The third key feature is the characteristic of stray light. For the wide-band spectrograph, the largest proportion of stray light comes from overlapping range with the high-order diffraction light. So the order sorting filter is an essential component and the DELTA's Linear Variable Order Sorting Filters (LVOSF) has been selected. The LVOSF can suppress more stray light than traditional long wave pass filter, because the cut-on wavelength moves together with the linear dispersion of the grating. Figure 4-a) shows the fitting curves between cut-off wavelength and the position on the LVOSF with 1st and 2nd order diffracted lights. Fitting curve data is gained from moving transmittance curves measurement of LVOSF by step of 1mm. The 1st and 2nd order diffracted lights are calculated from the grating equation and geometrical equation between components. Actually the effective cut-off edge range in the coated area is tuned from 350nm to 670nm.From figure 4, the LVOSF's position can be determined by matching with the CCD linear image sensor.

Though, the overlapping high-order diffraction has been removed by LVOSF. There is still non-negligible stray light which is mainly caused by scattering from the non-ideal behavior of the optical components (mirrors, slits, grating) and from higher-order diffractions of the grating. Stray light error is serious when measuring a very low level spectral component at some wavelength while there are high level components in other wavelength regions. It is a very important specification for solar spectral irradiance measurement. A spectral stray light correction method has been proposed by Kostkowski for a scanning monochromatic incident light into spectrograph by measuring monochromatic spectral line sources that do not have any emission other than the spectral line itself.

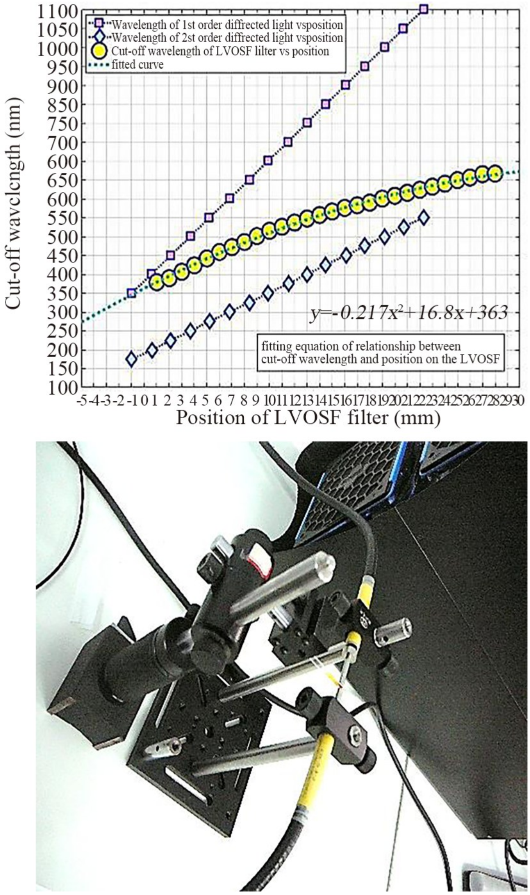

Fig. 4 a) Fitting curves between cut-off wavelength and the position on the LVOSF with 1st and 2nd order diffracted lights. b) Measurement of moving transmittance curves of LVOSF.

This method is based on the characterization of aspectrograph's slit scattering function (SSF), which is the relative spectral responsivity when the instrument is set at a fixed wavelength while the wavelength of the incident monochromatic source changes. The relationship that describes a spectrograph's relative response at every element i to a fixed monochromatic excitation at wavelength λj falling on the element $j = J$ is called the spectral line-spread function (LSF). Figure 5-a) shows the LSF matrix intensity map in log scale. The excitation wavelength is from 470nm to 890nm with a 10nm step. Figure 5-b) shows one LSF in matrix for $\lambda 23$, which means the excitation wavelength 700nm.

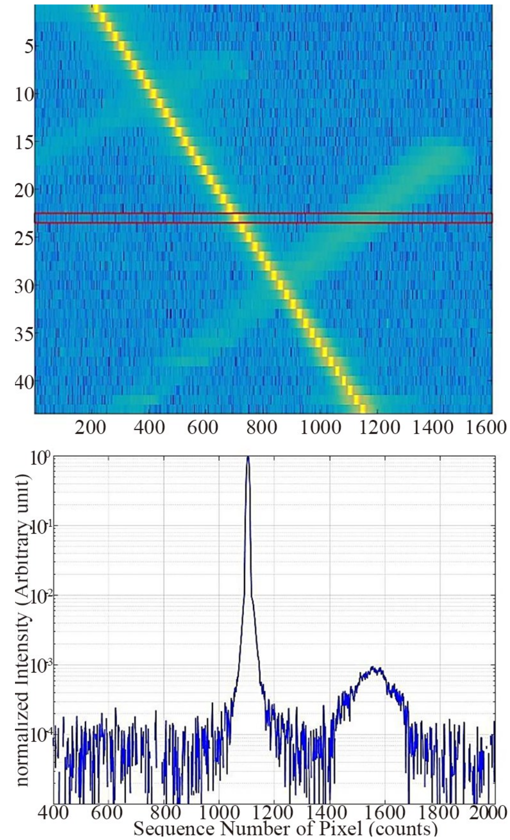

Fig. 5 a) LSF matrix intensity map in log scale. b) A typical LSF with excitation wavelength 700nm.

4 Spectral Specifications

There are 4 basic spectral specifications for a spectrograph including wavelength range, spectral resolution, wavelength interval and wavelength accuracy. The wavelength range of the spectrograph is from 300nm to 1100nm which is limited by the grating, the spectral response curve and image plane length of CCD sensor. The other 3 specifications can be fixed on by standard wavelength lamp measurement.

Calibrating the wavelength scale of the spectroradiometer typically involves measurement of lines at well-known wavelengths from a calibration lamp such as a mercury - argonlight source. This process is relatively straightforward when the lines are well separated, relative to the bandwidth of the spectrograph. The common method for wavelength calibration is the polynomial method. Coefficients in the polynomial that is used to express the corresponding relationship between wavelength and pixel position are obtained by polynomial fitting. The equation of wavelength calibration for fitting method can be summarized as:

$$\lambda_i = \sum_{j=0}^{n} a_j i^j i = 1,2,\cdots,N; j = 0,1\cdots,n \quad (1)$$

Where i is the sequence number of CCD's pixel, λ_i is the wavelength on the pixel i, j is the order of polynomial, a_j is the coefficient of this calibration equation. After wavelength calibration, the spectrum curve is shown in wavelength coordinate. The wavelength accuracy could be expressed by the residual error from calibration fitting. Table 1 shows the fitting residual of wavelength calibration by 12 specific wavelengths of Hg-Ar lamp with 5 order polynomial fitting. The absolute value of fitting residual is no more than 0.2nm. The calibration wavelength accuracy could be represented as ±0.2nm. So, wavelength interval is variable from 0.4nm to 0.44nm calculation by this polynomial fitting. It means that there are 4 or 5 pixels within FWHM at arbitrary wavelength.

Table 1 Fitting residual of wavelength calibration by 12 specific wavelengths of Hg-Ar lamp

Wavelength	313.155	404.656	546.074
No. of Pixel	166	372	687
Residual	0.0017	-0.0134	0.0251
Wavelength	696.543	763.511	772.376
No. of Pixel	1020	1168	1188
Residual	-0.0196	0.0038	-0.1731
Wavelength	794.818	826.452	912.297
No. of Pixel	1237	1307	1498
Residual	0.1230	0.1378	-0.1928
Wavelength	922.45	965.786	1013.976
No. of Pixel	1520	1616	1723
Residual	0.0404	0.088	-0.016
Polynomial fitting	$\lambda = 1.9944\times10^{-15} i^5 - 7.5294\times10^{-12} i^4 + 5.6579\times10^{-9} i^3 + 8.2506\times10^{-6} i^2 + 0.43913 i + 240.01$		

The spectral resolution generally is described by FWHM (Full Width at Half Maximum). The slit width is an essential factor in determining spectral resolution. The narrower the slit width is, the higher the spectral resolution of the mini-spectrograph is improved (just when slit width > PSF (Point spread function). Spectral resolution and throughput have a mutual trade-off. So the spectral resolution is an optional parameter by selecting different slit width. Figure 6-a) shows the spectrum of Hg-Ar lamp with 25um slit width in this optical bench. The FHWM at 4 typical specific wavelengths is shown in figure 6-b), which covers in almost full wavelength range. From figure 6-a), it can be seen that the FHWM is no more than 2nm by using 25um slit. A very close pair of adjacent peaks (576.96nm and 579.066) from spectrum of Hg-Ar lamp could be distinguished with this spectral resolution. This optical bench of spectrograph is good enough for solar irradiance observation.

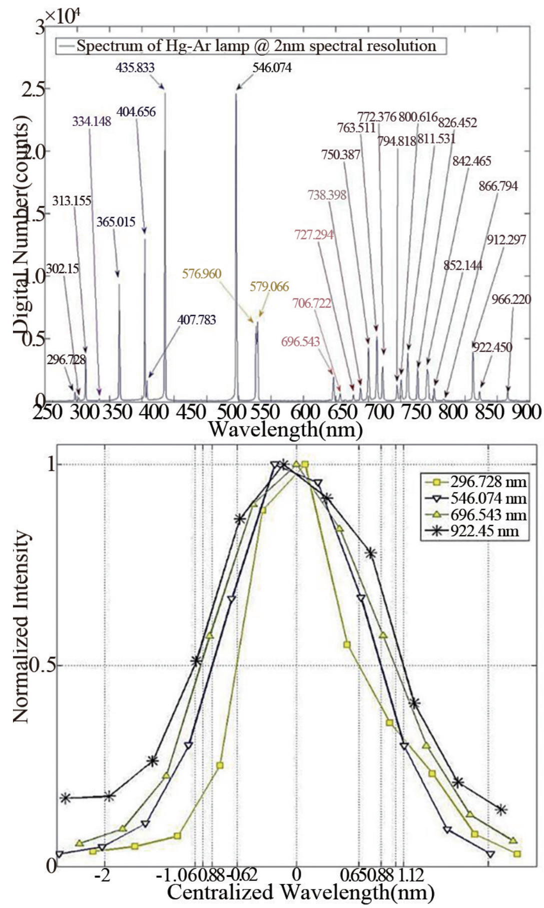

Fig. 6 a) Spectrum of Hg-Ar lamp. b) FHWM at4 typical specific wavelengths

5 Prototyping and Observation

GHI (Global Horizontal Irradiance) and DNI (Direct Normal Irradiance) are two basic forms for solar irradiance measurement defined in meteorological observation. GHI and DNI could be observed with hyperspectral resolution when this spectrograph is connected to the cosine corrector or telescopic aperture with a fiber. The hyperspectral resolution means that the λ/FWHM is on the order of 100. There are still two key technologies must be achieved before the spectrograph becomes to a spectroradiometer. One is the spectral irradiance traceability, and the other is fitness of environment for long-term unattended observation outdoors. Figure 7-a) shows the 3d model of solar spectroradiometer prototype. The solar spectroradiometer system also includes a humidity sensor and several temperature sensors to provide routine quality control information. The Peltier device is used to stabilize the temperature of CCD sensor to 25±1℃ by the dedicated Peltier driver and control circuit. Figure 7-b) shows the DNI type spectroradiometer working on the sun tracker.

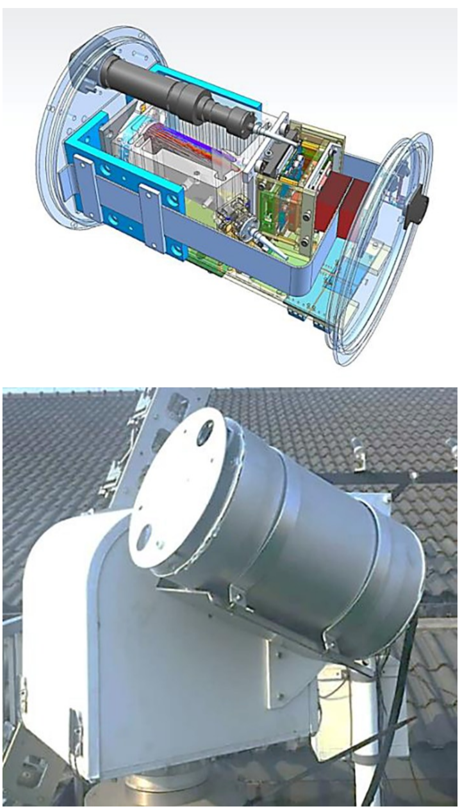

Fig. 7 a) 3d model of prototype. b) Prototype on the sun tracker.

The spectral data could give the irradiancein 1nm narrowband wavelength intervals. Figure 8-a)

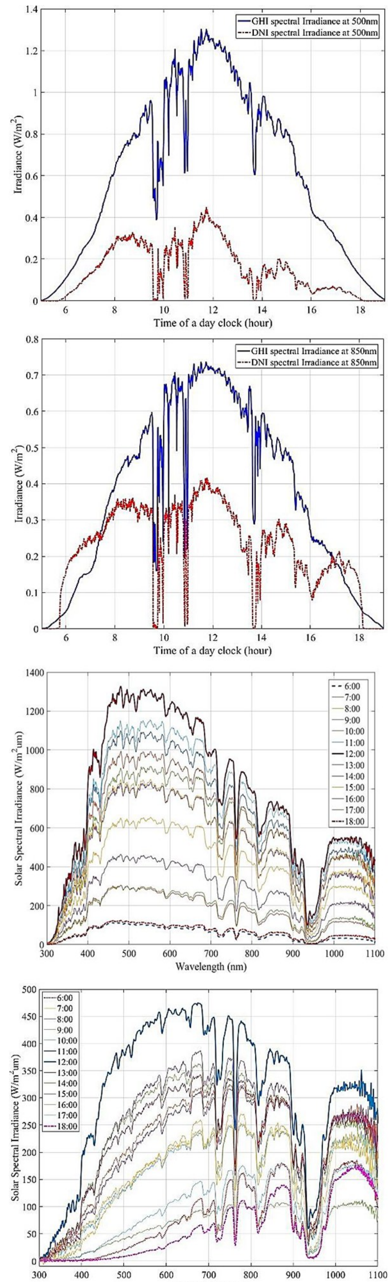

Fig. 8 a) Irradiance at 500nm of DNI and GHI. b) Irradiance at 850nm of DNI and GHI. c) Solar GHI spectral irradiance curves. d) Solar DNI spectral irradiance curves.

shows the DNI and GHI irradiance at 500nm. Figure 8-b) shows the DNI and GHI irradiance at 850nm. Especially, the spectral data could show the spectral power distribution of solar irradiance. Figure 8-c) shows the solar spectral irradiance curves observing by this GHI type spectroradiometer at one hour intervals for one day. Figure 8-d) shows the solar spectral irradiance curves observing by this DNI type spectroradiometer at one hour intervals for one day.

6 Conclusion

In conclusion, the solar spectroradiometer prototype has been designed and implemented in 2016. The spectral resolution has been estimated by the slit function. The spectral resolution is within2nm from 300nm to 1100nm by using 25um slit. And the calibration wavelength accuracy is within ±0.2nm and the wavelength interval is lightly larger than0.4nm. The spectral irradiance is traceable to the Division of Metrology in Optics and Laser, NIM (National Institute of Metrology, china).

Though, the solar spectroradiometer (include GHI type and DNI type) has been developed for meteorological observation, but the more accurate and precise calibration method of spectral irradiance is still a challenge for the wide dynamic range between the very bright sunlight at noon and the relatively much darker sunlight at sunset. And the adaptability of the climate and environment needs to be verified and optimized.

ACKNOWLEDGMENT

This work was supported from Meteorology Industry Research Special Funds for Public Welfare Projects (GYHY201406037).

References

[1] Hooker S B, Bernhard G, Morrow J H, et al (2012). Optical Sensors for Planetary Radiant Energy (OSPREy): Calibration and Validation of Current and Next-Generation NASA Missions. In: *International Conference on Renewable Energies and Power Quality*. [online] Hanover: ICREPQ, Vol.45, pp.588-593. Available at: http://www. sti. nasa. gov/STI-homepage. html/ [Accessed 31 Jul. 2012].

[2] Pacheco labrador J, Martín M P (2015). Characterization of a field spectroradiometer for unattended vegetation monitoring, Key sensor models and impacts on reflectance. *Sensors*, 15(2), pp.4154-4175.

[3] Osamu IJIMA (2012). The Temperature and Directional (Cosine) Responses of the Grating Spectroradiometer (MS-710). *Journal of Meteorological Research*, pp.37-42.

[4] Osamu IJIMA (2014). Observation of the Direct and Diffuse Spectral Solar Radiation using the Grating Spectroradiometer (MS-710). *Journal of Meteorological Research*, (72), pp.25-32.

[5] PMOD/WRC Annual Report, (2012).*Spectroradiometer for Spectral Aerosol Optical Depth and Solar Irradiance Measurements*. Davos: PMOD/WRC, p.13.

[6] PMOD/WRC Annual Report, (2013). *Instrument Scales*. Davos: PMOD/WRC, p.20.

[7] Feng Zheng, Liying Liu, Guoyu Zhang etc. (2015). Compact Spectrometer based on Concave Grating. In: *Proc. SPIE* 9795, *Proceedings of the Photoelectronic Technology Committee Conferences*. [online] Changchun: SPIE, Vol.9795, pp. 97951C1-4. Available at: http:// dx.doi.org/10.1117/12.2216023 [Accessed 11 Aug. 2015].

[8] Jiwu Chen, Wei Wang and Zhineng Li (2000). Design of a compact multichannel spectrophotometer using a holographic concave grating as dispersive element. In: *Proc. SPIE* 4223, *Instruments for Optics and Optoelectronic Inspection and Control.* [online] Beijing: SPIE, Vol.4223, pp.189-193. Available at: http://dx.doi.org/10.1117/12.401789 [Accessed 5 Oct. 2000].

[9] Chaoming Li, Xinrong Chen, Jianhong Wu and Zhuyuan Hu (2010). Micro-spectrometer based on flat field holographic concave grating. In: *Proc. SPIE* 7848, *Holography, Diffractive Optics, and Applications IV*. [online] Beijing: SPIE, Vol. 7848, pp. 78482C1-6. Available at: http:// dx.doi.org/10.1117/12.870076 [Accessed 17 Nov. 2010].

[10] Petr Hlubina and Pavel Stejskal (2002). Miniature fiber optic spectrometer: response functions and band passes. In: *Proc. SPIE* 4887, *Optical Techniques for Environmental Sensing, Workplace Safety, and Health*

Monitoring. [online] Warsaw: SPIE, Vol.4887, pp.1-10. Available at: http:// dx. doi. org/10. 1117/12. 475970 [Accessed 22 Jul. 2002].

Authors' Biographies

LIU Liying, born in 1981, is working for her Ph.D. degree at Faculty of Science in Changchun University of Science and Technology. She obtained her M.Sc. degree from the National Laboratory on High-Power Semiconductor Laser of Changchun University of Science and Technology. Her research interests include Spectroscopy and Imaging Science.

E-mail: liying_ivy@126.com

ZHENG Feng, born in 1981, is currently an R&D engineer in Jiangsu Radio Scientific Institute Co., LTD. He obtained his Ph.D. degree in Changchun University of Science and Technology in 2016. He has worked on data analysis and modeling in many application areas for many years, such as spectroscopy, radiometry, color science and chemometrics.

E-mail: zheng.feng@js1959.com